

# ACOUSTIC EMISSION FROM INTERNAL DELAMINATION OF A FOUR-PLY PLATE

E. Rhian Green

University of Leicester

Department of Engineering, Leicester LE1 7RH, U.K.

## INTRODUCTION

The basic inverse source problem of acoustic emission is the determination of the nature and location of the internal source from surface measurements of the transient elastic waves generated by the AE event. As pointed out by Sachse [1], this inverse problem requires a knowledge of the dynamic Green's function for the structure under examination. The evaluation of this dynamic Green's function is therefore a pivotal problem in the application of the techniques to monitor internal events in engineering structures. This paper deals with the determination of the transient motion of a four-ply fiber composite laminate resulting from an internal impulsive line load acting in the mid-plane of the plate in a direction normal to the mid-plane. The source function for acoustic emission associated with delamination will be located at one or other of the interfaces between the plies and the results presented here complement those of the earlier paper [2] which deals with an impulsive line load acting on the upper interface. Because of symmetry, the response to a line load at the lower interface may be deduced immediately from this upper interface solution.

The plate consists of four layers of a uni-directional fiber reinforced material, each of depth  $h$  but infinite lateral extent. Each lamina is modelled as a homogeneous, transversely isotropic elastic continuum with the axis of transverse isotropy lying in the plane of the lamina and parallel to the fiber direction. This continuum model will be invalid for short wavelengths due to the diffraction and scattering by individual fibers. Consequently, attention is restricted to wavelengths of the order of ten times the fiber diameter and inter fiber spacing. The laminae are perfectly bonded in a symmetric cross-ply configuration  $(0^\circ, 90^\circ)_s$ . In practice, there are resin-rich layers present between adjacent laminae which may be modelled by considering the transversely isotropic layer to be separated by viscoelastic isotropic layers (see e.g. Mal [3]). This effect has not been included in the theory presented here.

The response of single plates to internal sources has been examined by a number of authors. For an infinite plate of isotropic elastic material, Ceranoglu and Pao [4] have applied the generalised ray theory and Cagniard's method in

order to calculate the Green's dyadics. An alternative technique using expansions in normal modes is employed by Weaver and Pao [5], whilst Vaseduvan and Mal [6] use integral transform techniques to solve the problem. Enoki and Kishi [7] have developed a three dimensional finite difference method which they have applied to calculate the Green's function for a precracked tension specimen of finite dimensions. In the case of anisotropic elastic materials, the solution for a single plate has been derived by Willis and Bedding [8] and reference has already been made to the earlier work of the present author [2].

## THEORY

This is described in some detail in [2], thus only an outline of the method will be given here. A Cartesian coordinate system of axes is set up with the origin in the mid-plane, the  $x_1$  axis being normal to the plate and the  $x_2$  and  $x_3$  axes being parallel to the fibres in the two outer and two inner layers respectively. The line source is taken to be a delta function impulse acting at the mid-plane in the negative  $x_1$  direction at an angle  $\pi/2 - \gamma$  to the  $x_3$  - axis. The consequent plane wave propagation will be at an angle  $\gamma$  to the  $x_3$  - axis and parallel to the layers. Hence, each stress and displacement component at any time  $t$  may be expressed as functions of  $x_1$ ,  $x$  and  $t$  only, where  $x = x_2 \sin \gamma + x_3 \cos \gamma$ . It is convenient to take the Laplace transform with respect to  $t$  and the Fourier transform with respect to  $x$  of each of these components. Utilising the appropriate constitutive equations, the full three-dimensional equations of elasticity are solved for each layer. The ensuing solutions are subjected to the traction-free conditions appropriate to the two outer surfaces together with the perfect bonding conditions of continuity of stress and displacement at each interface, apart from the stress discontinuity at the mid-plane due to the impulsive loading.

Once all these conditions have been implemented it is possible to express the transformed stress and displacement components at any point on or within the plate in terms of the material constants, the propagation angle and the transform parameters. All that remains to derive the full solution to the problem is to invert the transforms in order to recover the stress and displacement components as functions of  $x$  and  $t$ . This inversion is carried out numerically using residue theory for the frequency inversion followed by integration along each branch of the dispersion equation. Due to the symmetry of the plate, any disturbance separates into two distinct motions, flexural (antisymmetric) and longitudinal (symmetric), with the advantage that the plate dispersion equation may be expressed as the product of two dispersion equations, one corresponding to the flexural motion and the other to the longitudinal. The numerical techniques are applied to the two motions separately and the full solutions are obtained upon using an appropriate combination of the two partial solutions. The limits of integration are chosen to be consistent with the continuum theory and the summation is restricted to ten branches of each of the two dispersion curves. However, for a source located at the mid-plane, the disturbance has no symmetric content but is purely antisymmetric. Thus, the numerical calculations are halved and the solutions appropriate to the lower half of the plate are identical to those for the upper half.

## DISCUSSION

A typical carbon fiber, epoxy resin composite material with the ratio of the

modulus along the fibers to that at right angles to the fibres of the order of 25 is chosen to provide the numerical values of the material constants necessary to generate the results. The response of the plate may be discussed with reference to the scaled normal displacement,  $u$ . The first four figures presented show the variation of  $u$  with the distance (measured in units of  $h$ ) from the line source at a fixed instant of time  $t = 200 h/c$  after the occurrence of the impulse. Here,  $c$  is the speed of a longitudinal wave travelling transverse to the fibers, thus  $t = 200 h/c$  is the time taken for this wave to travel through fifty plate thicknesses.

Though this paper is concerned in the main with the surface response to internal sources, and in particular to the surface response to a source located at the mid-plane, it is of interest to begin the discussion with a brief consideration of the through thickness response to such a source. Figures 1 and 2 show plots of the variation in  $u$  at three levels, namely the upper surface, upper interface and mid-plane. As stated earlier, the response on the lower interface and lower surface is identical to that on the upper interface and upper surface respectively. For figure 1,  $\gamma = 30^\circ$  and for figure 2,  $\gamma = 60^\circ$ . One of the interesting features is that both figures indicate that the high frequency effect is confined to the inner layers which is consistent with the location of the line source. This high frequency disturbance has travelled much further when  $\gamma = 30^\circ$  than when  $\gamma = 60^\circ$  which is to be expected since the quasi-shear wave speed in the inner layers at  $\gamma = 30^\circ$  is  $0.678c$  compared with  $0.555c$  when  $\gamma = 60^\circ$ . The corresponding distances away from the location of the pulse are  $x = 135.6h$  and  $x = 111h$  respectively. However, the amplitude of this high frequency motion is considerably smaller when  $\gamma = 30^\circ$  than when  $\gamma = 60^\circ$ . This reflects the fact that the effective Young's modulus of the material for propagation at  $30^\circ$  to the fibers is of the order of seven times that when the stress wave is propagating at the greater angle of  $60^\circ$  to the fibers. Thus, in the former case, the core layers appear stiffer and more constrained than in the latter case and the movement at the mid-plane is more inhibited. This interest in the high frequency response is due to the fact that the stresses are associated with the displacement gradients and will thus be high in regions of high frequency.

Since the main objective is to ascertain whether the location of the internal source may be predicted by monitoring the surface response, it is of interest to examine figures 3 and 4 corresponding to  $\gamma = 30^\circ$  and  $60^\circ$  respectively. They show the upper surface response to three different locations of the internal line source, namely the upper interface, the mid-plane and the lower interface. The downward displacement of the line on the upper surface immediately above the line source appears to depend on the depth of the source. For both angles of propagation, there is a definite increase in the initial amplitude of the sinusoidal disturbance as the source moves downwards through the plate. In each figure there is evidence that there is more of a high frequency content in the response to the source located at an interface between two different ply orientations than at an interface between two identical fiber directions. In fact, a source located at the mid-plane, i.e. at the greatest depth from a free surface, has a significantly quieter response than the other locations. There is evidence of a Rayleigh-type surface wave in figures 3a from the high amplitude oscillation present at a distance of  $x = 105h$ , (the Rayleigh wave speed is  $0.527c$ ), which distinguishes a source at the upper interface from that at the lower interface. However, there is no such apparent distinction between the corresponding figures 4a and 4c for  $\gamma = 60^\circ$ . This is consistent with earlier results [2] which predict that for the material parameters employed here, a surface wave will not exist for values of  $\gamma$

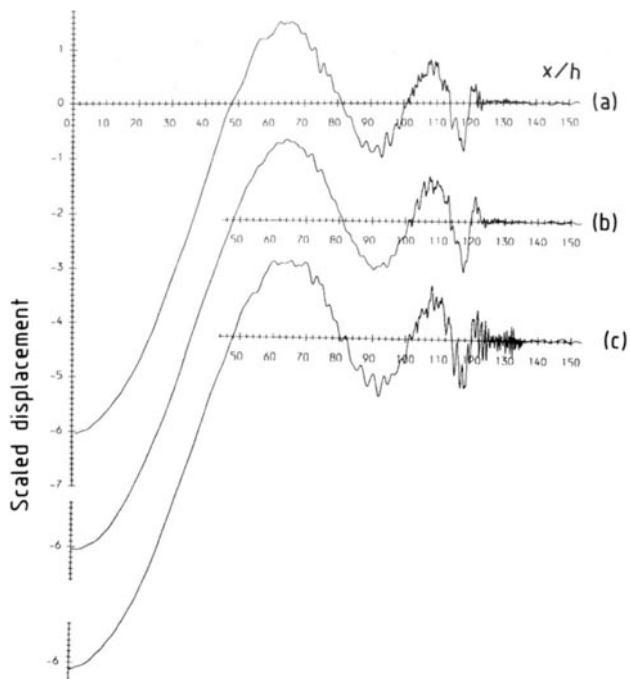


Fig. 1. Scaled normal displacement at  $t = 200 h/c$ ,  $\gamma = 30^\circ$ .  
 (a) Upper Surface (b) Upper Interface (c) Midplane

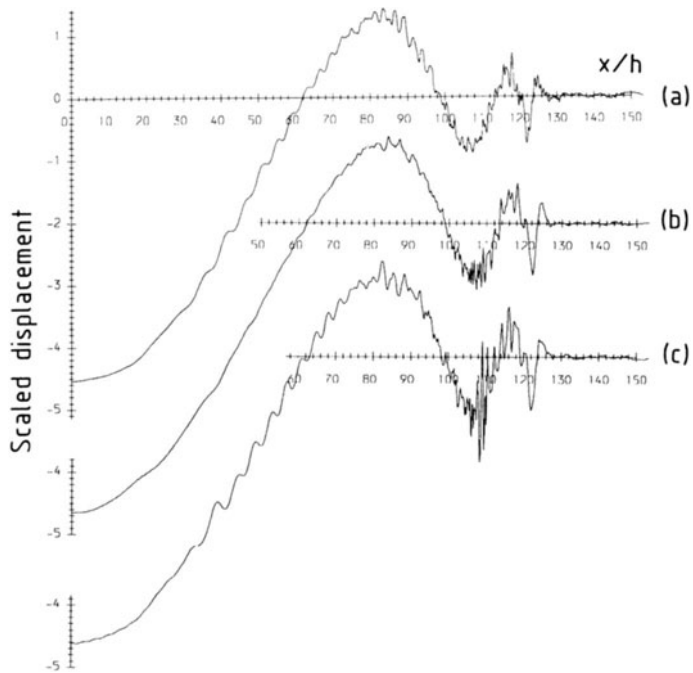


Fig. 2. Scaled normal displacement at  $t = 200 h/c$ ,  $\gamma = 60^\circ$ .  
 (a) Upper Surface (b) Upper Interface (c) Midplane

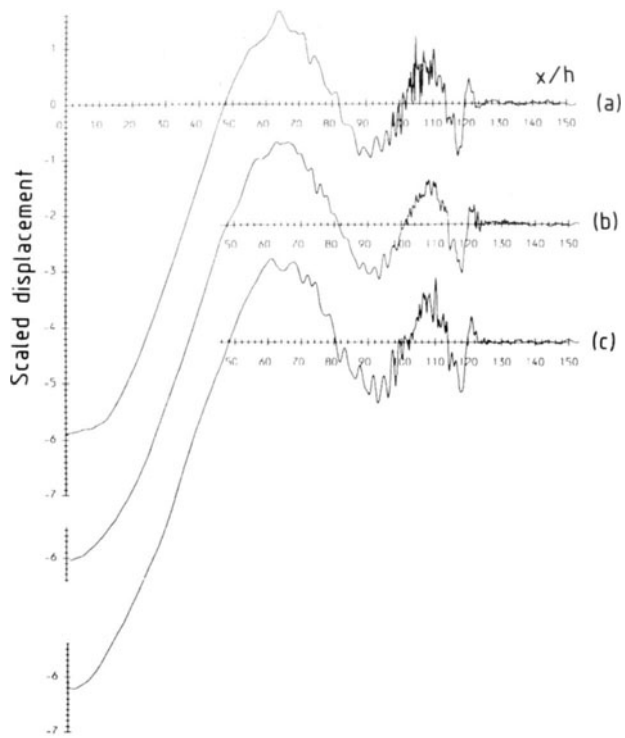


Fig. 3. Upper surface displacement at  $t = 200 h/c$ ,  $\gamma = 30^\circ$  due to source located at (a) Upper Interface (b) Midplane (c) Lower Interface

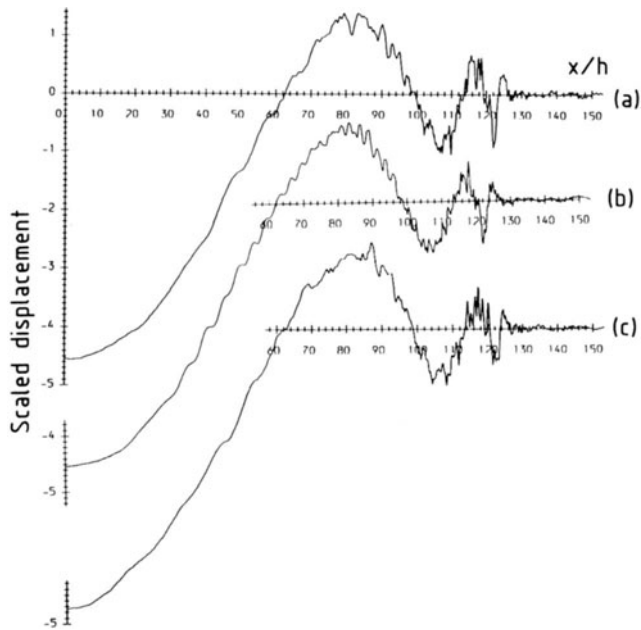


Fig. 4. Upper surface displacement at  $t = 200 h/c$ ,  $\gamma = 60^\circ$  due to source located at (a) Upper Interface (b) Midplane (c) Lower Interface

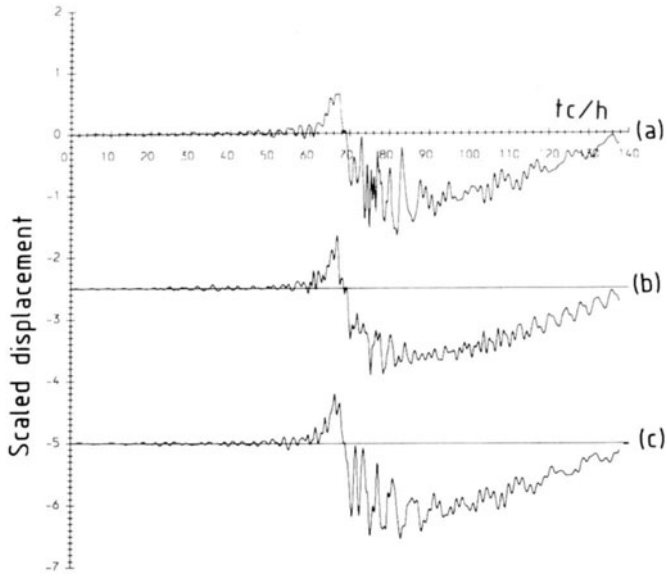


Fig. 5. Upper surface displacement at  $x = 40 h$ ,  $\gamma = 30^\circ$  due to source located at (a) Upper Interface (b) Midplane (c) Lower Interface

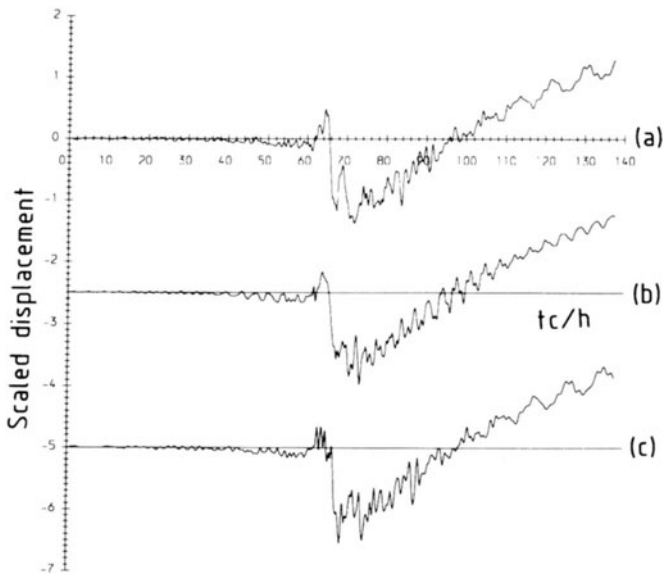


Fig. 6. Upper surface displacement at  $x = 40 h$ ,  $\gamma = 60^\circ$  due to source located at (a) Upper Interface (b) Midplane (c) Lower Interface

greater than  $47.6^\circ$ . The peaks and troughs of the response are more pronounced in figure 4a than in figure 4c. For example, the point on the surface at a distance of  $122h$  has been displaced almost twice as much by the upper interface source as by a source located at the lower interface.

In contrast to these four figures, which show the response of the plate at a fixed time, figures 5 and 6 show the passage of the plane wave through a particular point  $P$  on the upper surface.  $P$  is at a distance of  $40h$  from the line source and in figure 5,  $\gamma = 30^\circ$  and in figure 6,  $\gamma = 60^\circ$ . In each case, curves (a), (b) and (c) correspond to a source located at the upper interface, the midplane and lower interface respectively. Note that for ease of comparison, curve (b) has been displaced downwards through 2.5 units and curve (c) 5 units.

The most striking feature of these two figures is the sharp downward step in the normal displacement at  $t = 69h/c$  when  $\gamma = 30^\circ$  and  $t = 66h/c$  when  $\gamma = 60^\circ$ . This appears to be associated with a shearing deformation of the stiffer layers of the laminate rather than the simple bending motion displayed by an isotropic material. The oscillations superimposed on the rising portions of the curves which follow this step represent arrivals due to multiple reflections within the layers.

Once again, there is evidence of a Rayleigh-type, very high frequency surface disturbance in figure 5a at a time of  $76h/c$ , which is noticeably absent from figure 6a. However, it is clear that though the response to the three different source locations are not identical, it is by no means an easy task to distinguish between them. A comparison of the response due to a midplane source with a source at the upper or lower interface does suggest that the strength of the disturbance decreases with the distance of the source from a free surface. This fact might be utilized to give some indication of the location of an internal source.

#### Acknowledgement

I am grateful to the University of Leicester Research Board and to the SERC (Grant No. GR/F/74448) for financial support of this work.

#### REFERENCES

1. W. Sachse, in Elastic Waves and Ultrasonic Nondestructive Evaluation, edited by S.K. Datta, J.D. Achenbach and Y.S. Rajapakse (North Holland, Amsterdam 1990) p. 285.
2. E. Rhian Green, in Review of Progress in Quantitative Nondestructive Evaluation, edited by D.O. Thompson and D.E. Chimenti (Plenum Press, NY 1991) Vol. 10, p. 1399.
3. A.K. Mal, Int. J. Eng. Sci., Vol. 26 (1988) p.873.
4. A.N. Ceranoglu and Y.H. Pao, ASME Jour. App. Mech., Vol. 48 (1981) p. 125.
5. R.L. Weaver and Y.H. Pao, ASME Jour. App. Mech., Vol. 49 (1982) p. 821.
6. N. Vaseduvan and A.K. Mal, ASME Jour. App. Mech., Vol. 52 (1985) p. 356.
7. M. Enoki and T.Kishi, in Elastic Waves and Ultrasonic Nondestructive Evaluation, edited by S.K. Datta, J.D. Achenbach and Y.S. Rajapakse (North Holland, Amsterdam 1990) p. 307.
8. J.R. Willis and R.J. Bedding, in Modern Problems in Elastic Wave Propagation, edited by J. Miklowitz and J.D. Achenbach. (Wiley, NY 1978) p. 347.